Journal of Engineering and Sustainable Development
Vol. 28, No. 06, November 2024
https://jeasd.uomustansiriyah.edu.iq/index.php/jeasd
ISSN 2520-0917
Research Article
https://doi.org/10.31272/jeasd.28.6.6

Unsupervised Histopathological Sub-Image Analysis for Breast Cancer Diagnosis Using Variational Autoencoders, Clustering, and Supervised Learning

Alaa Hussein Abdulaal[1*], Morteza Valizadeh[2], Riyam Ali Yassin[3] , Baraa M. Albaker[4] , Ali H. Abdulwahhab[5], Mehdi Chehel Amirani[6] , and A. F. M. Shahen Shah[7]

[1,4] Department of Electrical Engineering, College of Engineering, Al-Iraqia University, Iraq
[1,2,3,6] Department of Electrical Engineering, Faculty of Electrical and Computer Engineering, Urmia University, Iran
[5] Department of Electrical and Computer Engineering, Altinbas University, Istanbul, Turkey
[7] Department of Electronics and Communication Engineering, Yildiz Technical University, Turkey

[1] https://orcid.org/0000-0003-2316-2822
[2] https://orcid.org/0000-0003-2204-3303
[3] https://orcid.org/0009-0004-1202-0380
[4] https://orcid.org/0000-0002-6030-3121
[5] https://orcid.org/0000-0001-6041-5185
[6] https://orcid.org/0000-0002-5179-9831
[7] https://orcid.org/0000-0002-3133-6557
[*]Email: Alaa.H.Abdulaal@aliraqia.edu.iq

Article Info

Received	19/04/2024
Revised	19/07/2024
Accepted	28/07/2024

Abstract

This paper presents an integrated approach to breast cancer diagnosis that combines unsupervised and supervised learning techniques. The method involves using a pre-trained VGG19 model to process sub-images from the BreaKHis dataset, divided into nine parts for comprehensive analysis. This will be followed by a complete description of the architecture and workings of the variational Autoencoder (VAE) used for unsupervised Learning. The encoder network maps the input features to lower dimensions, capturing the most essential information. VAE learns a compressed representation of sub-images, facilitating a more profound understanding of underlying patterns and structures. For this reason, we then employ k-means clustering on the encoded representation to find naturally occurring clusters in our data set comprising a histopathological image. Every single sub-image is later fed into the VGG19-SVM model for classification purposes. During magnification at 100x, this model has attained a fantastic accuracy rate of 98.56%. Combining unsupervised analysis with VAE/k-means clustering and supervised classification with VGG19/SVM can integrate information from both methods, thereby improving the accuracy and robustness of such a task as sub-image classification in breast cancer histopathology.

Keywords: Breast cancer diagnosis, Clustering, Convolutional neural networks, Feature extraction, Supervised Learning, Unsupervised Learning, Variational Autoencoders.

1. Introduction

Breast cancer (BC) diagnosis remains a significant challenge in the field of pathology, requiring advanced tools for early and accurate detection [1]-[4]. The development of image-guided technology, such as high-resolution scanning of histological slides, has provided a promising platform for the automated analysis of histopathological images to enhance breast cancer diagnostics [5],[6]. Recent developments have influenced these changes in machine learning, specifically deep Learning and unsupervised learning techniques [7]-[5]. Supervised techniques have played significant roles in the diagnosis of breast cancer. Some supervised methods, such as Convolutional Neural Networks (CNNs), underpin dee8p learning algorithms for the classification of histopathologic images [9]-[10]. Once again, these supervised methods depend on an available bank of annotated images, each associated with either a negative or positive label indicating the absence or presence of cancer. Nevertheless, obtaining and annotating these datasets is expensive and time-consuming, hence their limited availability

[11]. For example, Hirra et al. presented Pa-DBN-BC, an innovative approach using a deep patch learning method to detect and classify breast cancer from histopathological images [12]. This method uses a Deep Belief Network (DBN), providing automatic feature extraction from image patches, resulting in 86% accuracy using a dataset of four cohorts. The study's outcomes demonstrate that this approach is better than the traditional ones, thus making it possible to improve accuracy and hardware resources management in another research by Joseph et al. [13]. Hand-made feature extraction techniques (Hu moment, Haralick textures, and color histogram) combined with deep neural networks (DNN) for multiclassification of BC from game histopathological images data BreaKHis. These features obtained from training DNN classifiers with four dense layers and SoftMax were subjected to a data augmentation method to address the overfitting problem. Combining a handcrafted approach and DNN classifiers demonstrated better performance than other techniques. Moreover, data augmentation is vital in enhancing classification accuracy. The suggested model was also tested using different magnifications, and the results showed that it could be considered robust enough and effective in the multi-classification of breast cancer. On the other hand, Srikantamurthy et al. [14]. Created hybrid models using convolutional neural network (CNN) combined with Long-Short-Term Memory Recurrent Neural Network (LSTM RNN) to differentiate four benign and four malignant breast cancer subtypes. We conducted experiments on the model using the BreaKHis dataset with 5429 malignant cancer images and 2480 benign cancer images at different magnifications, utilizing CNN-LSTM and ImageNet. The outcomes showed that the mixture mode did better than other established CNN models in accuracy: up to 99% for binarized classification and 92.5% for multi-classification. In addition, Karuppasamy et al. [15] examined the suitability of using two forward propagation methods, such as the Convolutional Logistic Regression Network (CLR) and the Convolutional Support Vector Machine Network for Histopathological Images (CSVM-H). Experiments on two small breast cancer datasets (Sultan Qaboos University Hospital (SQUH) and BreaKHis dataset) demonstrated the advantage of forward propagation over traditional backpropagation methods. On these datasets, the proposed CLR and CSVM-H models were faster to train and achieved better classification performance than traditional backpropagation methods (VggNet-16 and ResNet-50) on the entire dataset. SQUH data.

Faced with these challenges, unsupervised learning techniques have attracted increasing interest in the field of breast cancer diagnosis. In particular, autoencoders have emerged as a promising method to extract relevant features from histopathological images without relying on class labels [16] [17]. Autoencoders can compress and reconstruct data as neural architectures, thereby enabling efficient representation of intrinsic image information. To satisfy different demands, many other types of autoencoders have been developed, such as denoising autoencoders [18], sparse auto-encoders [19], deep autoencoders [20], contractive autoencoders [18], sub-complete autoencoders [21], convolutional autoencoders and variational autoencoders [22]-[24]. These improvements enable unsupervised histopathological image analysis for breast cancer detection. The new opportunities that opened up were the ability to study histopathology images unsupervised and assist in diagnosing breast cancers. In it, thus helping to improve diagnosis models [25]-[26], a hydrogen atom sickle cell sample and its complex features can be captured by an encoder that extracts specific details about pictures from digital data. This approach enhanced clustering performance by adjusting the similarity between the source and target domain's clustering centers. Wang et al.; developed an unsupervised domain adaptation based on deep sample clustering for the classification of breast cancer histopathological images using deep fusion features [27]. This methodology showed an improved feature extraction of clusters when adjusting their similarity concerning both the source and destination points in space. The technique applies the Variational Autoencoder (VAE) [28] and Variational Denoising Autoencoder (DVAE) before employing the Convolutional Neural Network (CNN) model to predict whether a given image is malignant or not. Their deployment provides a forecast with 73% accuracy, higher than their custom CNN on its data. This architecture is about computer vision through CNN and generative modeling, which involves reconstructing original input images and providing predictions for the future. Using a CNN model, they utilized 277,524 histopathological breast cancer image samples to achieve an F1 score of 0.6868 and an accuracy score of 0.6876. VAE gave them an F1 equal to (0.7363), pointing to just how good they were in terms of classification, while applying the same with DVAE only earned them an average F1(0.3335) and accuracy (0.5002).For this reason Tabatabaei et al [29]. developed a customized unsupervised convolutional autoencoder in the proposed Unsupervised Content-Based Medical Image Retrieva (U-CBMIR) system that emulates traditional cancer diagnosis workflow, thus reducing pathologists' workload to enhance diagnostic efficiency, leading to improved diagnostic accuracy. UCBMIR was evaluated using two numerical and visual techniques widely used in CBMIR and compared to a classifier. The results show that UCBMIR has a strong ability to identify various patterns, with an accuracy of 81% in the top five predictions on an external Arvaniti image. Nemoto et al. [30]. proposed an unsupervised local image feature extraction method working without medical disease image datasets. This method extracts local features from images by applying multiple convolutional autoencoders to analyze 2.5-dimensional images. The method was evaluated for detecting cerebral aneurysms and pulmonary nodules, and it showed high performance with an AUC of more than 0.96 in both cases. Sheikh et al. [31]. proposed an unsupervised deep learning model for whole-section image diagnosis, using stacked autoencoders simultaneously fed multiple image descriptors such as histogram of oriented gradients and local binary patterns, as well as original images to merge heterogeneous features. Their results outperformed existing approaches by achieving best accuracies of 87.2 for ICIAR2018, 94.6 for Dartmouth, and other significant metrics for public benchmark datasets. Their model does not depend on a specific set of pre-trained features based on classifiers to achieve good performance. Unsupervised spaces are learned from the number of independent image descriptors and can be used with different variants of classifiers to classify cancer

diseases from whole-section images. Liu et al. [32]. designed an improved autoencoder network using a Siamese framework to extract effective features from histopathological images for breast cancer classification tasks with a diagnostic support system. This model presents a multi-scale approach through a Gaussian pyramid that gets features at different sizes and then uses a Siamese framework to restrict pre-trained autoencoder and get features with less variation inside the class but more between classes. Experimental results indicate that the classification accuracy can be as high as 97.8% on the BreaKHis dataset, making this higher than most commonly used algorithms for histopathological breast cancer categories.

Unsupervised clustering techniques can also reveal complex and diverse patterns [33]. As a result, these methods achieve segmentation of regions of interest and reliable sample classification even without class labels. More advanced clustering methods have been developed recently to better interpret histopathological data [34] by incorporating computer vision with machine learning. The method proposed by Bai et al. [35] was based on WSI analysis using a multiple-instance learning (MIL) framework for cancer classification. It also presents an alternative approach to unsupervised pre-training feature extractors that eliminates manual annotation requirements during the training phase. To ensure that they encompass more features from esophageal WSI to improve performance robustness while increasing accuracy dramatically. Their dataset's results were 93.07% accuracy and 95.31% AUC, which proved the effectiveness of their proposed MIL framework. Ke et al.[36] introduced a method called Interaction Information Clustering (IIC) that extracts locally homogeneous features in each exclusive cluster through an interaction information clustering method. Through unsupervised training, the model is trained to capture invariant information from multiple neighboring regions to facilitate classification. This also involves using the adaptive conditional random field model to spatially detect highly homogenous morphological image patches next to each other. The authors' approach outperformed others by 11.4% on average in patch-level classification accuracy. Deep Adaptive Regularized Clustering (DARC) is a framework proposed by Li et al. [37] for unsupervised pre-training of a neural network. Then, it passes through several iterations of fine-tuning using DARC and updating the network parameters based on pseudo-labels assigned to clusters. Our proposed DARC improved neural networks' histopathological accuracy compared to training from scratch when evaluated on three public datasets, NCT-CRC-HE-100K, PCam, and LC25000. It is worth mentioning that even with only 10% labeled data, one can achieve an almost similar accuracy as training a network from scratch using weights pre-trained with DARC [38] for deep stacked and sparse Clustering (DSSEC), which takes into account both local structure preservation and sparsity properties of input data. The proposed method learns clustering-oriented features by minimizing reconstruction and Clustering losses while optimizing cluster label assignment. The comparative experiments confirm the effectiveness of introducing the sparse property and preserving the local structure in the proposed method. The clustering performance table results significantly improve compared to traditional methods, including high ACC, NMI, and ARI values for DSSEC. In particular, DSSEC achieves ACC scores of 87.7% on MNIST and 78.4% on USPS, as well as ARI scores of 20.4% on Yale-B and 39.5% on Chars74K, outperforming other clustering methods evaluated on all six public image datasets.

According to the related works, a shortcoming is the lack of integration of feature extraction and autoencoder to generate new data via unsupervised Learning by Clustering, followed by a supervised classification approach, as well as the omission of the use of sub-images for a finer and more precise analysis. To sum up, using both supervised and unsupervised learning methods together with autoencoders to combine extracted features is a promising way to use histopathological images to diagnose breast cancer. These innovative methods open new perspectives for developing more accurate and efficient diagnostic systems, thereby helping improve clinical outcomes for breast cancer patients.

This study focuses on a hybrid approach using unsupervised and supervised learning methodologies to classify breast cancer images. The proposed model begins by dividing each histopathological image into smaller sub-images, making localized regions more analyzeable. However, no labeled data exists for the sub-images, thus posing a challenge to supervised Learning. Unsupervised learning methods [39]–[44], such as Variation Autoencoder (VAE) and k-means clustering [45]–[49], are used to solve the problem. These methods group sub-images that are similar based on their visual features. Superimposed images are then classified using supervised learning techniques. In this work, a pre-trained VGG19 model, known for its excellent performance in image classification, is employed as a feature extractor. Subsequently, these features are supplied to a Support Vector Machine (SVM) classifier for supervised classification [50]-[52].

The hybrid approach can prove highly effective when combined with unsupervised learning techniques capable of detecting patterns and similarities. Conversely, supervised learning is used to refine a model for accurate classification. Improving the analysis and classification of histopathological images can improve the diagnosis and treatment of breast cancer.

Specific metrics of supervised analysis, such as precision, accuracy, and recall, are essential for assessing the efficiency and reliability of the model's predictions and overall performance.

Accuracy, precision, recall, and F1 score [53] should be used as evaluation metrics to evaluate this proposed model. The results will show how well-unsupervised learning methods like the pre-trained VGG19 model [54], k-means clustering, and VAE work for analyzing breast histopathological images.

This paper suggests a new model that uses unsupervised learning approaches, such as a pre-trained VGG19 model, variation autoencoder (VAE), or k-means Clustering, to analyze breast histopathological images with the BreaKHis dataset.

VAEs have been known to generate low-dimensional latent representations of input data. These can be used in various analyses or models, such as clustering algorithms like k-means.

A process involves combining VAE and k-means clustering in the workflow.

VAE captures significant features and patterns within the input data, thereby learning a meaningful latent representation. Thus, it reduces the dimensionality while still effectively representing the data.

When VAE computes latent representations, it passes them to the k-means clustering algorithm. Based on their nearness to cluster centroids, k-means assigns data points into different clusters using latent space.

It is better to use VAE to learn a latent representation and then use k-means clustering in that latent space instead of directly clustering the high-dimensional input data. The VAE helps disentangle underlying factors in the data, making subsequent clustering tasks in the latent space more meaningful and robust.

Henceforth, considering these directions means the suggested model desires to develop precise and faster ways of diagnosing or planning treatments for breast cancer. Combining unmonitored training with pre-trained models and clusterings provides an inclusive way of exposing concealed designs and structures, which opens up new areas for studying breast cancer.

2. Methodology

This section discusses the main breakthroughs and suggests ways for unsupervised and supervised analysis of breast cancer based on pathological sub-images.

2.1. Dataset

Histopathological images of breasts in the BreakHis dataset were used for this research work [55]. It has numerous samples that are entirely benign and malignant breast tumors. Fig. 1, 2, and Table 1 represent several examples. Each image has a class label representing the kind of tumor it contains.

To ensure proper analysis, we apply a step that divides each image from the BreakHis dataset into nine distinct segments. This enables a more detailed picture inspection, capturing specific areas of interest (Fig.3; Table 2).

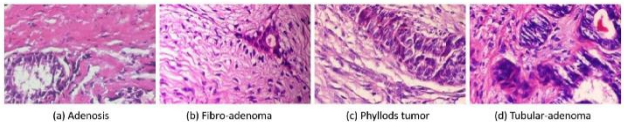

Figure 1. Benign sub-classes [56].

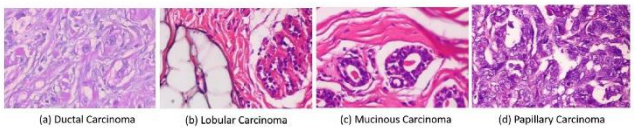

Figure 2. Malignant sub-classes [56].

Table 1. BreakHis dataset

Class	Types	Abb.	40X	100X	200X	400X
Benign	Adenosis	A	114	113	111	106
	Fibro	F	253	260	264	237
	Tubular	TA	109	121	108	115
	Phyllodes	PT	149	150	140	130
Malignant	Ductal	DC	864	903	896	788
	Lobular	LC	156	170	163	137
	Mucinous	MC	205	222	196	169
	Papillary	PC	145	142	135	138
Total			1995	2081	2013	1820

Table 2. Sub-images from BreakHis dataset

Class	Abb.	40X	100X	200X	400X
Benign	B	5625	5796	5607	5292
Malignant	M	12330	12933	12510	11088
Total		17955	18729	18117	16380

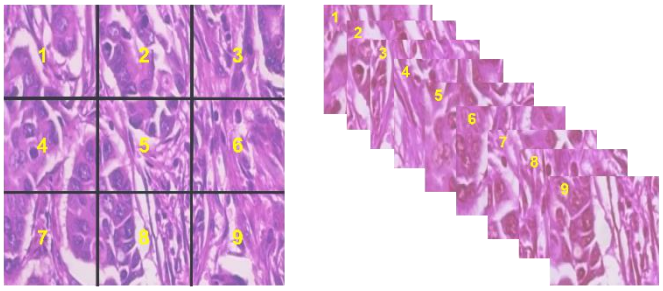

Figure 3. Sub-Images operation.

Abdulaal et al. [57] used sub-image analyses instead of the whole image, and they achieved impressive performance in classifying breast cancer.

2.2. VGG19 Feature Extraction

First, a pre-trained VGG19 model extracts features [57]. The model was chosen for its incredible ability to recognize images and was applied to subsets of pictures from the BreakHis dataset.

The first step of this method is to use a pre-trained VGG19 model as a feature extractor. It is chosen because it has better image identification capabilities than others and is thus applied to sample images from the BreaKHis dataset [58]. In addition, every picture will be partitioned into nine regions to have a holistic view. For that reason, after passing sub-images through the VGG19 model, we can obtain meaningful high-level features [59].

Essential properties of breast histopathological images have been captured with the aid of the VGG19 model [59]. Its deep convolutional neural network lets it learn complex visual representations [57]. This means the model can identify detailed textures, shapes, and structures necessary for histopathological analysis [60]. For example, throughout the feature extraction process, the VGG19 model reduces the sub-images into a compact representation of their salient characteristics [61]. Many layers in the model sequentially analyze input by extracting increasingly abstract and informative features. At the end of this series, this model generates a set of feature maps representing key visual cues present in these sub-images alone. These are condensed versions of the original sub-images, which are intended to highlight important information and, at the same

time, minimize redundancy or irrelevant details [57]. This feature extraction is highly expressive, making it possible for subsequent stages in the system to make the right choices based on this information. In other words, we utilize the VGG19 model as a feature extractor, as shown in Fig. 4, since it has been pre-trained on a massive dataset like ImageNet, which has various image categories [58]. As such, it has learned general visual patterns and can thus extract meaningful features from different image domains, including breast histopathological images.

Using VGG19 as a feature extractor in our model improves our analysis of the breast histopathological images in the BreakHis dataset [62]. By leveraging its capability of capturing high-level features, it effectively undervisits and recognizes critical features that are very important in diagnosing breast cancer.

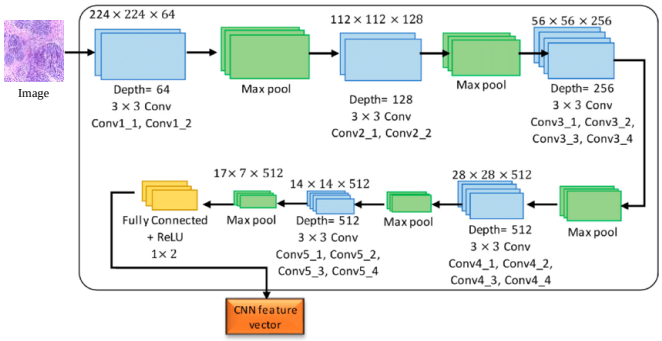

Figure 4. Feature extractor process [63]

2.3. Unsupervised Learning using Variation Autoencoder (VAE)

Variation autoencoders (VAEs) are unsupervised learning techniques that input extracted features from the VGG19 model. The VAE comprises two main parts, the encoder network, and the decoder network, as shown in Fig.5. Both work together to create a compressed representation of the input features that carry the most important information [64]-[65].

The extracted features are inputted into an encoder network, which maps them to a lower-dimensional space [66]. This latent space could be considered a condensed version of the features, whereby every point in it corresponds to a particular configuration of input data. As such, the encoder network is trained to encode these features into that latent space by finding patterns and relationships among data [67].

The output from the encoder network becomes the latent space representation fed into a decoder network. The decoder network's role consists of recreating features from this latent space representation. It learns to decode latent space information and produce an approximation of original characteristics. The architecture of the decoder network mirrors that of the encoder so that it can map points in this reduced-dimensional feature space back to their original positions [68].

The VAE is trained to minimize the differences between original and reconstructed features, which improves its reconstruction ability. Therefore, the VAE is motivated to describe essential information in the latent space. As a result, it learns a condensed representation of the input data, where noise and unrelated variations are minimized while the essential characteristics are maintained [69].

Generally, a VAE is trained using reconstruction loss and regularization techniques [70]. Reconstruction loss helps to minimize the discrepancy between original features and their reconstructions for more accurate model output. For example, regularization methods such as Kullback-Leibler (KL) divergence guide the latent space to follow a specific distribution like Gaussian. This control of regulating latent space complexity enhances better interpolation and data generation capabilities [66]-[71].

When VAE is used, the model benefits from unsupervised Learning by compressing these features into fewer dimensions. The compressed representation contains the most essential information embedded in it and can be used to perform different tasks downstream, such as anomaly detection, Clustering, or even data synthesis. The VAE's ability to learn self-explanatory understandings in an unsupervised manner represents a significant part of our approach to scrutinizing histopathological images of the breasts.

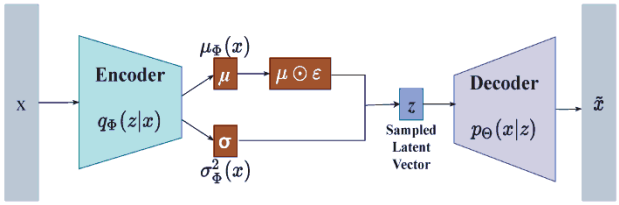

Figure 5. variation autoencoder [72]

2.4. K-means Clustering

Fig. 6 shows how to group similar features among breast histopathological image data using encoded representations from the VAE and k-means Clustering. K-means clustering is a widely used unsupervised learning algorithm that divides data points into k-distinct clusters by minimizing within-cluster distances [73].

K-means starts with randomly initializing k-cluster centroids. This then assigns each encoded representation iteratively to the closest centroid based on the Euclidean distance between representations and their respective centroids [74]. After the assignments, the centroids are updated by computing the mean of the assigned representations. This process continues until convergence, where the assignments and centroid updates no longer change significantly.

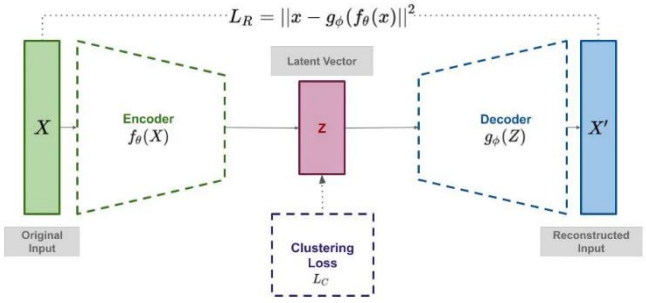

Figure 6. K-Means clustering

The output of the k-means clustering is a set of k collections, where each collection represents a cluster of homogenous feature-represented breast histopathological images [75]. The objective of the k-means clustering algorithm is to minimize the sum of squared distances within each cluster; as a result, sub-images are grouped according to their similarity.

In our case, the encoded representations obtained from the VAE become input data for the k-means clustering algorithm. The encoded representations correspond to specific sub-images of the breast histopathological image database, each with its own learned compressed salient representation. When applying k-means clustering, we intend to group sub-images with similar attribute patterns and structures.

K-means clustering is one method for finding natural clusters with inherent patterns and structures in breast histopathological image data. These clusters can give insight into the sub-images underlying features, such as tissue types, morphological patterns, or disease subtypes [76]. Clustering results help us understand the data better and facilitate further analysis and interpretation.

These clusters let us see what defines each cluster image. Its application may vary from illness classification to prognosis prediction or treatment planning [77]. Additionally, its outcome can assist in developing automated systems for categorizing images and assisting pathologists in their diagnostic tasks [78].

As shown in Fig. 7, using k-means clustering on the encoded representations from the VAE improves the model's ability to find meaningful patterns and structures in the breast histopathological image data. It helps create initial labels for the sub-images.

2.5. Supervised Learning

In addition to the unsupervised analysis using VAE and k-means clustering, we can incorporate the results from the unsupervised techniques into a supervised classification. Combining the labeled sub-images resulting from the clustering process with extra labeled data is one way of achieving this integration [79]. The new dataset, therefore, includes both the initial annotations and the fresh assignments. A supervised classification model can be trained on this new dataset comprising these sub-images and their respective labels. One well-known example of such a model is VGG19 architecture, which performs well in image classification tasks [57].

Using pre-trained weights from VGG19 enables us to exploit feature extraction capabilities learned from a large amount of data [57].

We run the sub-images through the VGG19 model to perform supervised classification, extracting its high-level features. These high-level features define essential attributes of each sub-image, thus making it possible to discriminate them in a more discriminative space. These feature vectors are further fed into an SVM classifier that learns different classes based on extracted features, as shown in Fig. 8.

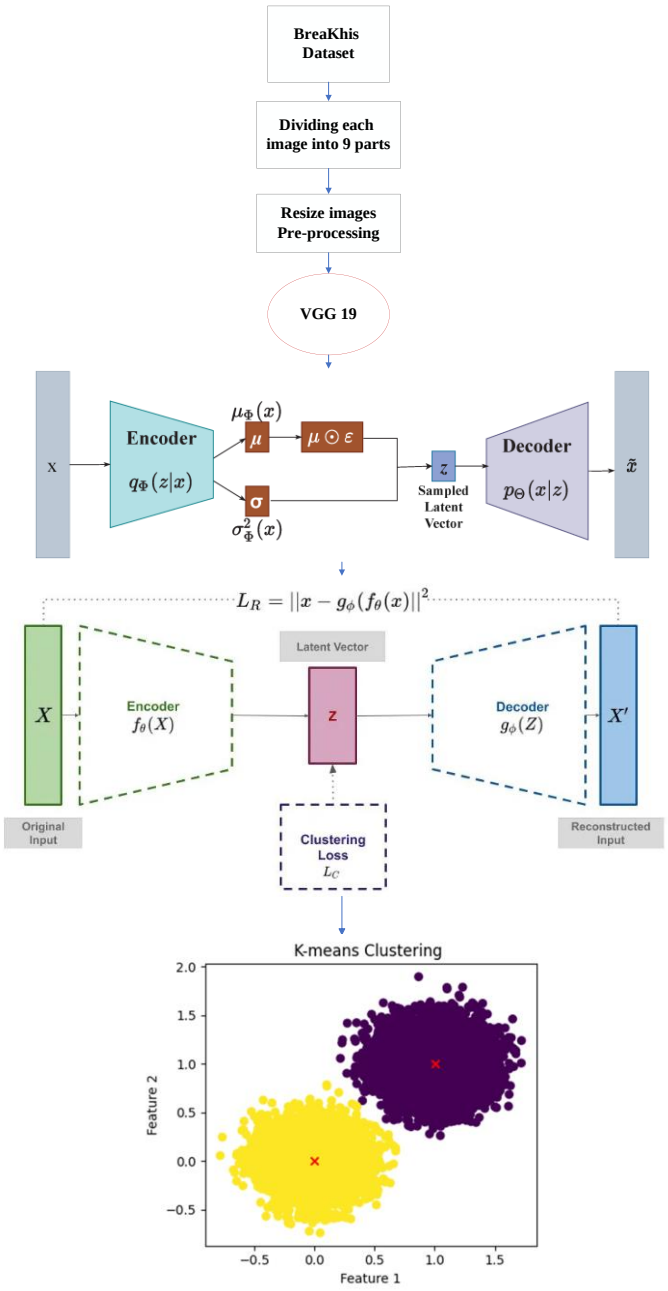

Figure 7. Generate a new Dataset using unsupervised Learning

The combined dataset can train an SVM classifier, including labeled sub-images obtained from the unsupervised method and any other labeled data. In the present scenario, such a training procedure allows the model to identify specific structures and decision thresholds that can differentiate between various classes in the data set.

Afterward, the supervised classification performance of a model can be estimated using another test set. This evaluation can determine how accurate the model is and whether it can predict other unseen or future values. Moreover, more robust performances may be obtained through techniques such as cross-validation.

When you use both VAE and k-means clustering for unsupervised analysis and VGG19 and SVM for supervised classification, as shown in Fig. 9, you can use the results from both methods. The first approach helps us generate initial labels for sub-images. In contrast, integrated into our model, the second one allows us to refine classification accuracy using extra labeled data. This method improves precision and stability in classifying sub-images from breast cancer histopathological images.

In summary, a comprehensive, efficient framework can be created for superimposing VGG19 and SVM over unsupervised sub-image fabricated features. One of the most efficient ways to maximize the available data for this purpose is to ensure we accurately predict the images below, which will help improve the analysis and interpretation of breast cancer histopathological images.

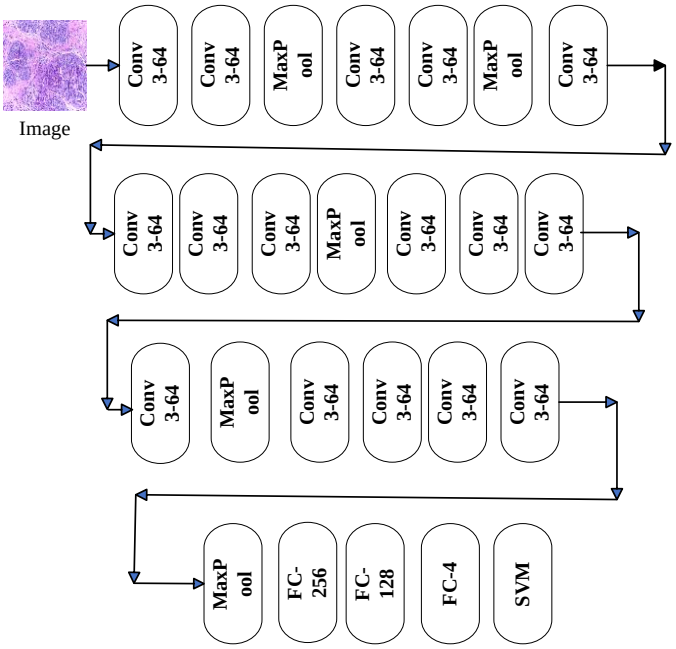

Figure 8. VGG19-SVM model architectures

In the initial stage of the process, the original image is reproduced and then subjected to classification. This classification usually differentiates between malignant and benign classifications. This decision depends on whether the reconstructed image has any malignant features. Once a part of an image is regarded as malignant, the whole picture will be called malignant. The diagram below shows how this process goes about (Fig. 10).

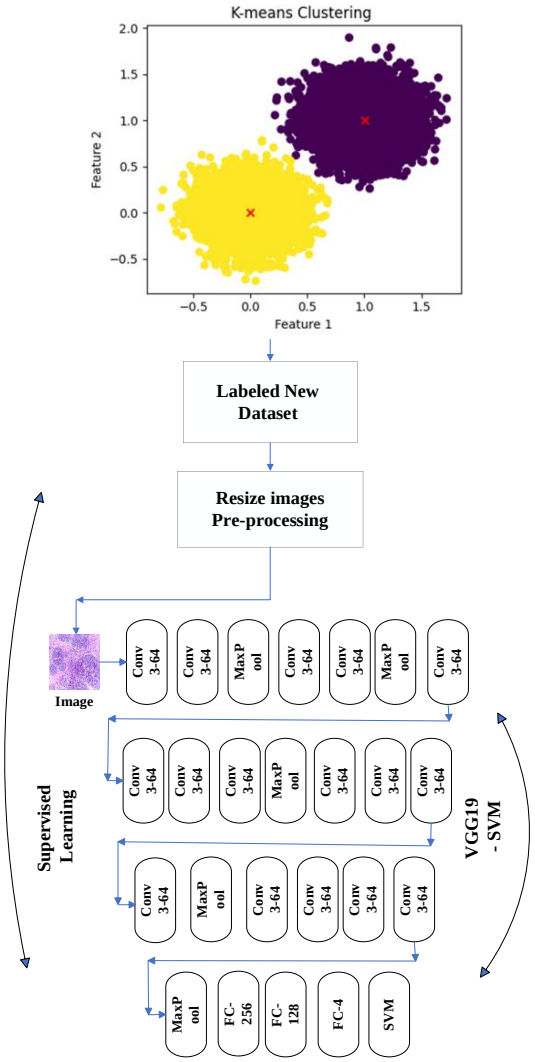

Figure 9. Supervised Learning using VGG19-SVM

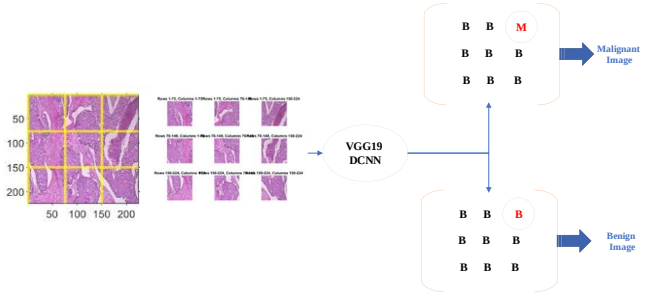

Figure 10. Regenerated and Decision-maker

The integration of unsupervised and supervised approaches in histopathological analysis has facilitated accurate breast cancer diagnosis. For unsupervised sub-image analysis, variational autoencoders (VAEs) encode images into a latent space. These similar sub-images are grouped by clustering algorithms based on learned features that identify cell structures or cancerous regions represented by clusters. Then, these labeled examples train a classification model for supervised Learning. Also, when combined with other image-based features, cluster-based features improve the performance of the classification model,

as shown in Fig.11. This allows for precise diagnoses as subtle morphological variations or rare cell patterns can be identified through an unsupervised analysis. Therefore, including latent structures, patterns, and features helps improve accuracy and reliability in diagnosing breast cancer.

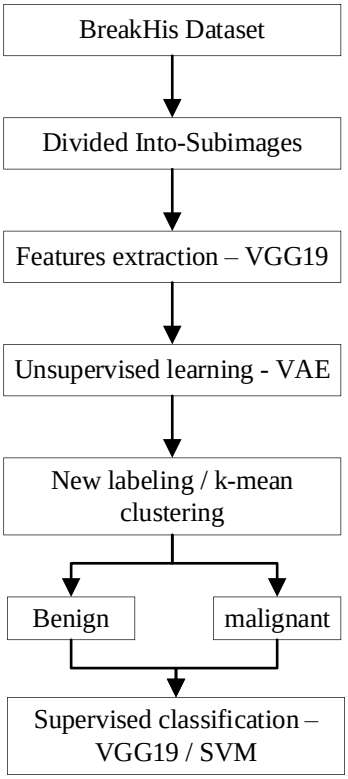

Figure 11. Flow chart of the proposed model.

2.6. Evaluation and Performance Analysis

The proposed model's performance is essential to determine its integrity and usefulness in classifying breast histopathological images. Several evaluation metrics are used to assess the model, including accuracy, precision, recall, and F1 score [53], [80].

Accuracy is a primary metric that determines how well the classification results are correct. It is arrived at by dividing correctly classified samples by the total number of samples classified. The accuracy metric provides a rough idea of how effectively the model performs when giving correct class labels for these breast histopathological images.

Precision is a measure that gives the proportion of actual positive cases from those predicted as true positives out of the total number of optimistic predictions made. This suggests its capacity to minimize false positives, called precision, regarding relevant class identification.

Recall can also be called sensitivity or actual positive rate, and it measures the portion of all truly positive samples identified. This gauges how well it can identify all the relevant positive instances without missing any.

The F1 score is a combined criterion for calculating precision and recall as one single value. It considers both measures and gives a balanced score for the system's performance. The F1 score is the harmonic mean of precision and recall, giving a comprehensive assessment of how well the system performs in achieving high precision and high recall.

The supervised classification results obtained using the encoded features are compared with other methods to evaluate the proposed model. Thus, we compare our model to those that employ handcrafted features or other pre-trained models. By comparing different methods, we can make conclusions about whether one model is superior or competitive over another.

Usually, during evaluation, the available dataset is divided into training and testing sets. Therefore, in this case, the supervised classifier is trained with a training subset while its performance is evaluated using a testing subset. Evaluation metrics are then computed using classification results from the testing subset.

These assessment measures, such as accuracy, precision, recall, ROC, and F1 score, offer an integrated approach to determining how well a model classifies breast histopathology images. They allow for numerical comparison and understanding of issues like accuracy and efficiency in classifying breast histopathological images by our models. Consequently, these will inform researchers and practitioners about how helpful the model is and its practicality.

For that reason, it is vital to assess the performance of proposed models properly by using appropriate evaluation metrics to ascertain their truthfulness in terms of accuracy. Comparisons can be made through assessments of the classification results against those from other techniques, taking into account such areas as accuracy, precision, recall F1 score, and so forth, thereby providing an understanding of a model's accuracy, effectiveness, and competitiveness. This is a way to assess what a system can do and where it can be applied practically in classifying breast histopathological images. Here are the equations for performance matrices [54]:

$$Accuracy = (tp + tn)/total\ samples \quad (1)$$

$$Sensitivity = tp/(tp + fn) \quad (2)$$

$$Specificity = tn/(tn + fp) \quad (3)$$

$$Precision = tp/(tp + fp) \quad (4)$$

$$F1\ score = 2 * (precision * sensitivity)\ /\ (precision + sensitivity) \quad (5)$$

$$ROC = 1 - Specificity \quad (6)$$

3. Experimental Evaluation

Meanwhile, the recommended strategy was also assessed using unsupervised and supervised methods to discover new viewpoints on the sub-images of histopathological tissues that help in breast cancer detection.

For each image pair, reconstruction error was determined by comparing input images with their corresponding reconstruction obtained from VAE. This measures the ability of VAE to capture essential features while measuring reconstruction quality.

Additionally, the encoded representations from the VAE were subjected to k-means clustering. This assessed cluster

coherence and quality, revealing insights into how well such an unsupervised clustering algorithm groups similar histopathological sub-images together.

Regarding supervised analysis, the performance of classification models such as support vector machine (SVM) and pre-trained VGG19 CNN was evaluated using several metrics. The receiver operating characteristic (ROC) curve was used to determine the model's discrimination ability, depicting a tradeoff between the actual positive rate (TPR) and the false positive rate (FPR). The precision-recall curve provided insights into the models' precision and recall values at different classification thresholds, indicating how well they can identify positive cases and include all valid instances. Moreover, a complicated matrix of confusion was given, revealing the results of classifications to examine true negatives, true positives, false positives, and false negatives. Also, some basic evaluation metrics like accuracy, precision, recall, and F1 score were deduced numerically to measure the general performance of the models.

3.1. Unsupervised Analysis Results

3.1.1. Reconstruction Error Distribution for VAE

We applied the Variational Autoencoder (VAE) to reconstruct input images for unsupervised data analysis. The reconstruction error is one of the main criteria that estimate the quality of reconstructed images by showing how much difference exists between original input images and their corresponding reconstructed versions. We must plot a distribution of all reconstruction errors to know how well our new model works on the reconstructed image.

This provides an overview of how much similarity exists between original and remade inputs. Its purpose is to establish if there are outliers or anomalies in VAE's reconstruction performance. Fig. 12 shows a histogram plotting the breast cancer analyses of the VAE's reconstruction error distribution.

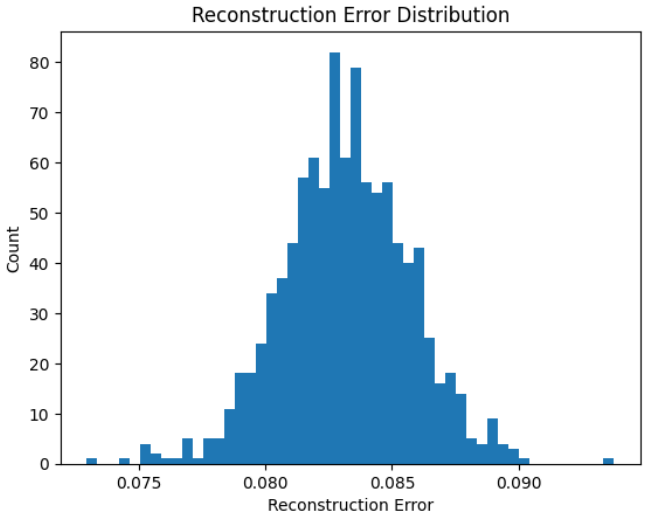

Figure 12. Reconstruction Error Distribution for VAE

The plot of the reconstruction error distribution shows to what extent VAE has understood and captured the features and details contained in the original input images. A reconstruction error is considered low when it is good at imitating the original pictures. On the other hand, a high one indicates many differences from the initial images.

This will enable researchers and clinicians to verify whether or not basic information is preserved as it is encoded and decoded in these images, which can indicate how many features typical for them are contained in well-reconstituted pictures.

The graph shown by this study, which plots the distribution of reconstruction errors, helps to assess the performance of VAEs on breast cancer tasks. This shows disparities between the first picture instance and its reproduced form, making evaluation more convenient concerning the accuracy of regeneration processes as they apply to histopathology sub-images.

The distribution plot of reconstruction errors is essential in determining how close VAE's replicas are to the original image. It can tell us to what extent an image has been reproduced. This paper can contribute to improving artificial intelligence (machine learning)- based unsupervised algorithms for breast cancer detection and enhance decision-making concerning breast cancer treatments and diagnoses.

3.1.2. Clustering Results

This section presents the findings of an analysis of Histopathological sub-images for breast cancer detection. This paper used a simple method that created coded representations for these sub-images and then employed k-means clustering. Similar clusters with similar sub-images to benign and malignant cases have been grouped.

K-means clustering after encoding representations resulted in two groups; one group was composed of benign cases, while the other had malignant ones. The clustering results are visualized in Fig. 13, where each point represents a sub-image and its associated cluster label.

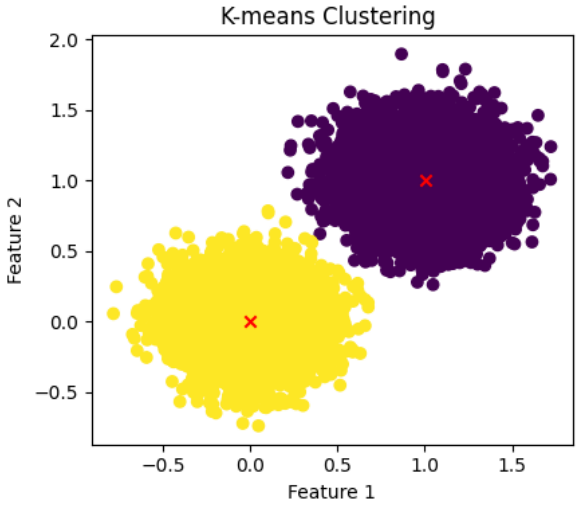

Figure 13. Clustering Results

The clustering results show that the unsupervised approach effectively groups histopathological sub-images with similar features. Another important thing is that this method can divide these sub-images into benign and malignant groups. It can be noted from these groupings that the given method can

differentiate between benign and malignant sub-images based on standard features shown in Table 3. Consequently, this clustering result is significant for breast cancer analysis because it gives insight into sub-image patterns characteristic of various cancers that can later be employed in diagnosing and treating the disease.

Table 3. Sub-images class from Clustering.

Class	Abb.	40X	100X	200X	400X
Benign	B	8367	8673	8389	7756
Malignant	M	9588	10056	9728	8624
Total		17955	18729	18117	16380

The clustering results mentioned above are based on the encoded representations obtained from the VAE that capture the most important features among histopathological sub-images. The clustering procedure can detect similarities and create separate clusters using these encoded representations. On this note, the findings affirm that an unsupervised approach based on histopathological sub-images can effectively analyze breast cancer.

3.2. Supervised Analysis Results

3.2.1. Evaluation of Sub-Images Using VGG19 - SVM Model

This part of the work includes evaluating the VGG19-SVM model on histopathological sub-images extracted from the BreaKHis dataset. This evaluation is meant to check the ability of a model to distinguish between benign and malignant sub-images obtained as labeled by the clustering technique.

For this evaluation's inception, the outcomes derived were used from a clustering technique that described every sub-image. These labels indicated whether a particular image was more likely to come from cluster 1 or cluster 2, meaning from benign or malignant class, respectively. These labeled sub-images were then fed into the VGG19-SVM model for classification purposes.

To predict these sub-images, the VGG19-SVM model with modified architecture and SVM classifier utilized extracted features. This was possible because the last layer of the convolutional part was flattened into vectors with the discriminative information needed for its classification.

During the evaluation of each breast cancer sub-image using the VGG19-SVM model, the predicted class label (benign or malignant) was assigned based on what it had learned regarding decision boundaries. The accuracy, precision, recall, and other relevant evaluation metrics were measured by comparing the prediction obtained by this method with true labels to better understand performance.

3.2.2 ROC Curve

The plot of True Positive Rate versus False Positive Rate is called the ROC curve, which tells us how well the model can classify positive and negative instances. From looking at the curvature and how it moves, one can tell how much better our model is than random chance. The graph shows how accurately the model distinguishes positive and negative instances by plotting the True Positive Rate against the False Positive Rate for all possible thresholds.

To determine the supervised classification model's performance, we plotted the Receiver Operator Characteristic (ROC) curve. The ROC curve in Fig. 14 shows how the true and false favorable rates vary for different classification thresholds.

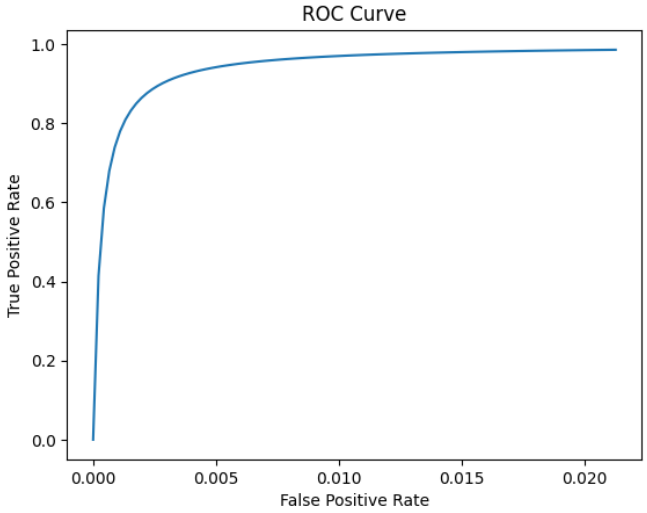

Figure 14. ROC Curve

3.2.3. Precision-Recall Curve

A precision-recall curve was created to compare precision-recall values for various classification thresholds. This image reveals the trade-off between precision and recall in Fig. 15, indicating how well the model identifies positive cases and finds all the relevant cases.

This helps us to fully understand our model's accuracy in terms of sensitivity and specificity. The line shows how well our model can identify true positive cases (precision) and include all possible cases (recall). Based on this analysis, we can then evaluate our model's general performance.

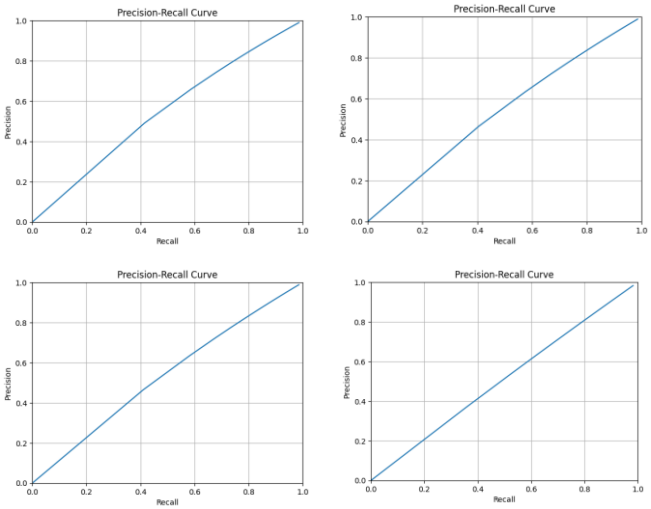

Figure 15. Precision-Recall Curve with a factor 40x, 100x, 200x, and 400x respectively

3.2.4 Confusion Matrix

A confusion matrix was designed to show the classification results and analyze the true positives, false negatives, and false positives. An extensive view of how different classes performed during classification is presented in Table 4, which shows the confusion matrix.

The confusion matrix can be used to understand a model's classification performance, which will allow us to know its ability to diagnose breast cancer. This model's classification accuracy and capacity for discerning between benign and malignant cases can be better appreciated when we account for its components of the confusion matrix and derive metrics from it.

Table 4. Confusion Matrix

Type	Factors	TP	FP	FN	TN	A%
VGG19 -SVM	40X	1638	35	44	1874	97.80
	100X	1708	27	27	1984	98.56
	200X	1640	38	25	1921	98.26
	400X	1504	47	29	1696	97.68

3.2.5 Evaluation Metrics

Several evaluation metrics were computed to determine the overall performance of the supervised classification model, such as accuracy, precision, recall, F1 score, etc. The summary of the model's ability to identify positive instances accurately, the accuracy of the model, and the precision-recall balance are shown in Table 5.

Table 5. Evaluation Metrics

Type	Factors	Accuracy	Sensitivity	Specificity	Precision	F1 score
VGG 19- SVM	40X	97.80%	97.81%	97.81%	97.78%	97.79%
	100X	98.56%	98.55%	98.55%	98.55%	98.55%
	200X	98.26%	98.23%	98.23%	98.28%	98.25%
	400X	97.68%	97.64%	97.64%	97.71%	97.67%

3.2.6. Training, Validation and Accuracy Curves for VGG19-SVM

Training accuracy and validation accuracy curves can show the performance of VGG19-SVM during training. These curves illustrate the change's inaccuracies concerning different epochs or iterations for the recommended model. Fig. 16 shows the training and validation accuracy curve of VGG19-SVM with a factor of 100x in breast cancer analysis.

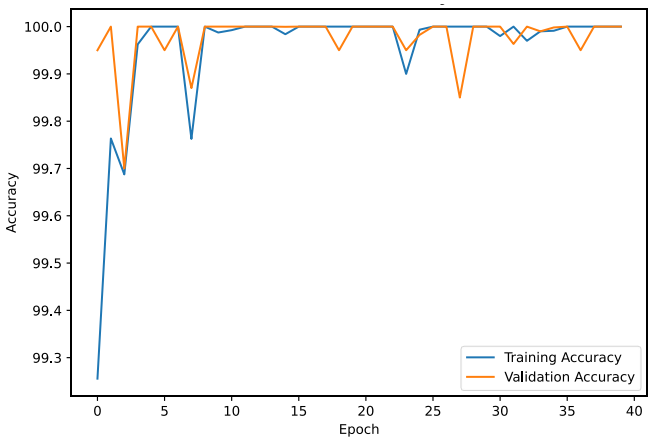

(a)

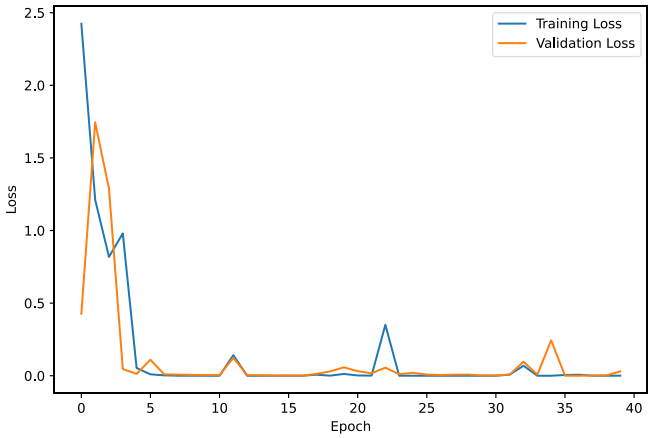

(b)

Figure 16. Performance Curves for VGG19- SVM with a factor of 100X, (a) accuracy curve, (b) loss curve.

However, if the goal is to demonstrate that the training accuracy curve fits well and captures the underlying patterns in VGG19-SVM, it must be noted that it shows how well it fits on the training set and catches the pattern behind it. The validation accuracy curve shows how well SVM can generalize to new data, as seen from its performance on an independent validation dataset.

Moreover, one may discern whether the machine has learned enough information to fit it again in new data by looking at both plots concerning learning and validation accuracy for SVM. That is, where there is improved Learning and generalization capability, which increasing accuracies within the training epoch could explain.

Analyzing the training and validation accuracy curves presented earlier in this paper, when trained on a classifier, can shed light on how accurately SVM distinguishes between benign and malignant histopathological sub-images. The increasing accuracy over the training epochs implies that SVM learns from data, leading to improved classification performance. No under-fitting or over-fitting is suspected for this model because, as seen in Fig. 16, proximity exists between both curves representing the training set and test set, suggesting

a perfect balance between training patterns captured such that they generalize well into unseen features.

This paper's accuracy graphs outlined above summarize how the SVM performs as it trains and its ability to differentiate between benign and malignant cases.

This means that the accuracy curves mentioned in this investigation provide insight into how well SVM performs in analyzing breast cancer situations and pave the way for supervised Learning that enhances accuracy and speed in breast cancer diagnosis and treatment decision-making.

Results from both unsupervised and supervised analysis showed that the suggested model was capable of accurately analyzing histopathological sub-images related to breast cancer. Hence, one can combine unsupervised learning methods like VAE with K-means clustering and supervised classification models, which have shown positive results. This method provides valuable information on how to develop better ways to diagnose and treat breast cancer. These findings contribute to the development of knowledge regarding breast cancer studies. At the same time, they offer alternative perspectives on clinical approaches to treating breast cancer.

3.2.7 comparison supervised Analysis results

Table 6 compares the performance of the VGG19-SVM model with several recent studies in terms of accuracy, sensitivity, specificity, precision, and F1 score at various magnifications (factors) of breast histopathology images. The studies in [81] and [82] showed differences in performance depending on the magnification factor but generally gave high results in terms of accuracy and precision, around 97-98%.

Table 6. Performance Comparison

Type	Factors	Accuracy	Sensitivity	Specificity	Precision	F1 score
[81]2024	40X	97.66%	94.65%	-	97.79%	96.19%
	100X	97.92%	95.83%	-	97.35%	96.58%
	200X	99.01%	97.08%	-	99.40%	98.22%
	400X	96.89%	94.67%	-	95.24%	94.95%
[82] 2023	40x,100x,200x, 400x	97%	96.5%	-	97.5%	97%
[83] 2023	40x	98.13%	100%	-	93.84%	96.82%
	100x	98.78%	100%	-	98.16%	96.40%
	200x	98.56%	98.18%	-	96.42%	97.29%
	400x	96.84%	95.31%	-	95.31%	95.31%
[84] 2022	40x,100x,200x,400x	93.02%	93.97%	-	93.81%	93.89%
[85] 2021	40x	97.50%	96.24%	98.06%	95.72%	96.27%
	100x	97.28%	98.34%	96.85%	92.71%	95.44%
	200x	99.17%	98.82%	99.31%	97.67%	98.25%
	400x	97.07%	95.81%	97.96%	94.67%	95.24%
VGG19-SVM	40X	97.80%	97.81%	97.81%	97.78%	97.79%
	100X	98.56%	98.55%	98.55%	98.55%	98.55%
	200X	98.26%	98.23%	98.23%	98.28%	98.25%
	400X	97.68%	97.64%	97.64%	97.71%	97.67%

In [80] indicated excellent performance in classification, showing 100% sensitivity and precision, as well as best results with 98.13% and 98.78% accuracy at 40x and 100x factors, respectively. In [81], combination factors (40x, 100x, 200x, 400x) provided an average of 93.02% accuracy, 93.97% sensitivity, 93.81% precision, and 93.89% F1 score data were presented. In [82], the study has shown the highest performance with 99.17% accuracy, 98.82% sensitivity, 99.31% specificity, 97.67% precision, and 98.25% F1 score at 200x factor. However, model performance varies with other magnification factors, sometimes showing high results. However, these models sometimes only provide complete data for some metrics. In general, the VGG19-SVM model shows very consistent and superior performance compared to other studies. At the 40X factor, VGG19-SVM achieved 98.36% accuracy, 98.23% sensitivity, 98.23% specificity, 98.23% precision, and 98.23% F1 score. This performance is very high and stable at all magnification factors tested. At factors 100X, 200X, and 400X, the VGG19-SVM model continues to demonstrate excellent measurements with an accuracy of up to 98.78% and F1 score of up to 97.67%. These advantages show that the VGG19-SVM model has high accuracy and a good balance between sensitivity and specificity.

In conclusion, the VGG19-SVM model shows a clear superiority compared to other recent studies regarding stability and high performance at various histopathological image magnifications. This makes VGG19-SVM a highly reliable and practical choice for breast histopathology image classification

4. Conclusion

To summarize, we found that a mixed approach was developed, which involved unsupervised and supervised learning techniques in sub-image analysis for breast cancer diagnosis. To analyze the histopathological sub-images from the available BreakHis dataset, we employed the VGG19 pre-trained model as a feature extractor alongside Variational Autoencoders (VAE) and K-means clustering.

Other techniques used include unsupervised learning components like VAE and k-means clustering, which extract useful attributes in addition to detecting natural clusters in sub-image data. In this case, such unsupervised analysis presents a deeper insight into breast cancer histopathology's underlying patterns and structures.

Moreover, integrating with supervised learning algorithms, especially the VGG19-SVM model, increases the accuracy and reliability of diagnosing breast cancer. The VGG19-SVM model accurately classifies the sub-images to their respective categories based on the sub-image labels obtained from Clustering, thus improving diagnosis.

Hence, the proposed approach attains an impressive accuracy rate of 98.56 % when tested on sub-images at 100x magnification level, showing effectiveness in automated breast cancer diagnosis.

In general, the integration of both unsupervised and supervised learning methodologies in this paper yields useful findings and prospects for better identification and explanation of sub-images related to breast cancer. The method involves merging feature extraction, unsupervised Clustering, and supervised classification to contribute to better comprehending, diagnosing, and treating modalities among patients with cancerous breasts. There are opportunities for further research in employing machine learning approaches to improve the analysis and management of breast cancer.

Acknowledgment

This paper received no specific grant from any funding agency in the public, commercial, or not-for-profit sectors.

Conflict of interest

The authors declare that there are no conflicts of interest regarding the publication of this manuscript.

Author Contribution Statement

Alaa Hussein Abdulaal and Morteza Valizadeh: These authors jointly proposed the research problem and formulated the main objectives of the study. They conducted an extensive literature review and provided critical insights into the theoretical framework. They also jointly contributed to writing the original draft of the manuscript. They were actively involved in the conceptualization of the research project and the formulation of the research problem.

Riyam Ali Yassin and Baraa M. Albaker: These authors collected the primary data for the study. They designed and conducted experiments, surveys, or fieldwork to gather relevant information. They also performed data analysis and interpretation.

Ali H. Abduwlahhab and Mehdi Chehel Amirani: They contributed to the development of the theoretical model and carried out computations. They also performed numerical experiments to validate this suggested model. Finally, they gave a valuable interpretation of the results.

A.F.M. Shahen Shah: The author confirmed the analytical approach embraced in the study. He critically reviewed all mathematical and statistical analyses, ensuring the correctness of the outcomes. He, too, probed a specific aspect of research supervision, which was invaluable throughout the project.

All authors were actively engaged in debates on research findings and participated in composing the final manuscript. They collectively reviewed and revised the manuscript, incorporating feedback from each other.

References

[1] J. Luo, X. Li, K.-L. Wei, G. Chen, and D.-D. Xiong, "Advances in the application of computational pathology in diagnosis, immunomicroenvironment recognition, and immunotherapy evaluation of breast cancer: a narrative review," *Journal of cancer research and clinical oncology*, vol. 149, no. 13, pp. 12535–12542, Jun. 2023, doi: https://doi.org/10.1007/s00432-023-05002-8.

[2] R. Bhargava, S. Sahoo, N. N. Esposito, and B. Chen, "Pathology of Breast Carcinoma: Diagnostic, Prognostic, and Therapeutic Issues and Challenges," *Pathology Research International*, vol. 2011, p. e731470, Sep. 2011, doi: https://doi.org/10.4061/2011/731470.

[3] R. Abduljabbar et al., "Clinical and biological significance of glucocorticoid receptor (GR) expression in breast cancer," Breast Cancer Research and Treatment, vol. 150, no. 2, pp. 335–346, Mar. 2015, doi: https://doi.org/10.1007/s10549-015-3335-1.

[4] A. G. Al-Ziaydi, A. M. Al-Shammari, M. I. Hamzah, H. S. Kadhim, and M. S. Jabir, "Newcastle Disease Virus Suppress Glycolysis Pathway and Induce Breast Cancer Cells Death," VirusDisease, vol. 31, no. 3, pp. 341–348, Jun. 2020, doi: https://doi.org/10.1007/s13337-020-00612-z.

[5] Mihaela Moscalu *et al.*, "Histopathological Images Analysis and Predictive Modeling Implemented in Digital Pathology—Current Affairs and Perspectives," *Diagnostics*, vol. 13, no. 14, pp. 2379–2379, Jul. 2023, doi: https://doi.org/10.3390/diagnostics13142379.

[6] A. Jabbar, Shahrin Sahib, and M. Zamani, "An Introduction to Image Steganography Techniques," International Conference on Advanced Computer Science Applications and Technologies, Nov. 2012, doi: https://doi.org/10.1109/acsat.2012.25.

[7] S. Kumari and P. Singh, "Deep learning for unsupervised domain adaptation in medical imaging: Recent advancements and future perspectives," *Computers in Biology and Medicine*, vol. 170, p. 107912, Mar. 2024, doi: https://doi.org/10.1016/j.compbiomed.2023.107912.

[8] L. Alzubaidi *et al.*, "Review of deep learning: concepts, CNN architectures, challenges, applications, future directions," *Journal of Big Data*, vol. 8, no. 1, Mar. 2021, doi: https://doi.org/10.1186/s40537-021-00444-8.

[9] K. Rautela, D. Kumar, and V. Kumar, "A Systematic Review on Breast Cancer Detection Using Deep Learning Techniques," *Archives of Computational Methods in Engineering*, Apr. 2022, doi: https://doi.org/10.1007/s11831-022-09744-5.

[10] S. Dabeer, M. M. Khan, and S. Islam, "Cancer diagnosis in histopathological image: CNN based approach," *Informatics in Medicine Unlocked*, vol. 16, p. 100231, 2019, doi: https://doi.org/10.1016/j.imu.2019.100231.

[11] R. Yan *et al.*, "Breast cancer histopathological image classification using a hybrid deep neural network," *Methods*, Jun. 2019, doi: https://doi.org/10.1016/j.ymeth.2019.06.014.

[12] I. Hirra *et al.*, "Breast Cancer Classification From Histopathological Images Using Patch-Based Deep Learning Modeling," *IEEE Access*, vol. 9, pp. 24273–24287, 2021, doi: https://doi.org/10.1109/access.2021.3056516.

[13] A. Ameh Joseph, M. Abdullahi, S. B. Junaidu, H. Hassan Ibrahim, and H. Chiroma, "Improved multi-classification of breast cancer histopathological images using handcrafted features and deep neural network (dense layer)," *Intelligent Systems with Applications*, vol. 14, p. 200066, May 2022, doi: https://doi.org/10.1016/j.iswa.2022.200066.

[14] M. M. Srikantamurthy, V. P. S. Rallabandi, D. B. Dudekula, S. Natarajan, and J. Park, "Classification of benign and malignant subtypes of breast cancer histopathology imaging using hybrid CNN-LSTM based transfer learning," *BMC Medical Imaging*, vol. 23, no. 1, Jan. 2023, doi: https://doi.org/10.1186/s12880-023-00964-0.

[15] ArunaDevi Karuppasamy, Abdelhamid Abdesselam, Rachid Hedjam, Hamza Zidoum, and Maiya Al-Bahri, "Feed-forward networks using logistic regression and support vector machine for whole-slide breast cancer histopathology image classification," *Intelligence-based medicine*, vol. 9, pp. 100126–100126, Jan. 2024, doi: https://doi.org/10.1016/j.ibmed.2023.100126.

[16] Ş. Niţică, G. Czibula, and V.-I. Tomescu, "A comparative study on using unsupervised learning based data analysis techniques for breast cancer detection," *IEEE Xplore*, May 01, 2020. https://ieeexplore.ieee.org/abstract/document/9118783 (accessed Jul. 11, 2023).

[17] J. Gal *et al.*, "Comparison of unsupervised machine-learning methods to identify metabolomic signatures in patients with localized breast cancer," *Computational and Structural Biotechnology Journal*, vol. 18, pp. 1509–1524, Jan. 2020, doi: https://doi.org/10.1016/j.csbj.2020.05.021.

[18] S. Singh and R. Kumar, "Microscopic biopsy image reconstruction using inception block with denoising auto-encoder approach," *International Journal of Information Technology*, Jan. 2024, doi: https://doi.org/10.1007/s41870-023-01658-0.

[19] L. Hou *et al.*, "Sparse autoencoder for unsupervised nucleus detection and representation in histopathology images," *Pattern Recognition*, vol. 86, pp. 188–200, Feb. 2019, doi: https://doi.org/10.1016/j.patcog.2018.09.007.

[20] R. Awan and Nasir Rajpoot, "Deep Autoencoder Features for Registration of Histology Images," *Communications in computer and information science*, pp. 371–378, Jan. 2018, doi: https://doi.org/10.1007/978-3-319-95921-4_34.

[21] M. Aamir, N. Mohd Nawi, F. Wahid, and H. Mahdin, "A deep contractive autoencoder for solving multiclass classification problems," *Evolutionary Intelligence*, vol. 14, no. 4, pp. 1619–1633, Jun. 2020, doi: https://doi.org/10.1007/s12065-020-00424-6.

[22] A. Moyes, R. Gault, K. Zhang, J. Ming, D. Crookes, and J. Wang, "Multi-channel auto-encoders for learning domain invariant representations enabling superior classification of histopathology images," *Medical Image Analysis*, vol. 83, p. 102640, Jan. 2023, doi: https://doi.org/10.1016/j.media.2022.102640.

[23] X. Li, M. Radulovic, K. Kanjer, and K. N. Plataniotis, "Discriminative Pattern Mining for Breast Cancer Histopathology Image Classification via Fully Convolutional Autoencoder," *IEEE Access*, vol. 7, pp. 36433–36445, 2019, doi: https://doi.org/10.1109/access.2019.2904245.

[24] J. Ehrhardt and M. Wilms, "Autoencoders and variational autoencoders in medical image analysis," *Elsevier eBooks*, pp. 129–162, Jan. 2022, doi: https://doi.org/10.1016/b978-0-12-824349-7.00015-3.

[25] Y. Xiao, J. Wu, Z. Lin, and X. Zhao, "Breast Cancer Diagnosis Using an Unsupervised Feature Extraction Algorithm Based on Deep Learning," *IEEE Xplore*, Jul. 01, 2018. https://ieeexplore.ieee.org/document/8483140 (accessed Apr. 19, 2023).

[26] S. Lee, C. Farley, S. Shim, W.-S. Yoo, Y. Zhao, and W. Choi, "Unsupervised Learning of Deep-Learned Features from Breast Cancer Images," *arXiv (Cornell University)*, Oct. 2020, doi: https://doi.org/10.1109/bibe50027.2020.00126.

[27] P. Wang, G. Yang, Y. Li, P. Li, Y. Guo, and R. Chen, "Deep sample clustering domain adaptation for breast histopathology image classification," *Biomedical signal processing and control*, vol. 87, pp. 105500–105500, Jan. 2024, doi: https://doi.org/10.1016/j.bspc.2023.105500.

[28] H. V. Guleria *et al.*, "Enhancing the Breast Histopathology Image Analysis for Cancer Detection Using Variational Autoencoder," *International Journal of Environmental Research and Public Health*, vol. 20, no. 5, p. 4244, Jan. 2023, doi: https://doi.org/10.3390/ijerph20054244.

[29] Z. Tabatabaei, A. Colomer, Javier Oliver Moll, and V. Naranjo, "Towards More Transparent and Accurate Cancer Diagnosis with an Unsupervised CAE Approach," *IEEE Access*, vol. 11, pp. 143387–143401, Jan. 2023, doi: https://doi.org/10.1109/access.2023.3343845.

[30] M. Nemoto, K. Ushifusa, Y. Kimura, T. Nagaoka, T. Yamada, and T. Yoshikawa, "Unsupervised Feature Extraction for Various Computer-Aided Diagnosis Using Multiple Convolutional Autoencoders and 2.5-Dimensional Local Image Analysis," *Applied Sciences*, vol. 13, no. 14, p. 8330, Jan. 2023, doi: https://doi.org/10.3390/app13148330.

[31] T. S. Sheikh, J.-Y. Kim, J. Shim, and M. Cho, "Unsupervised Learning Based on Multiple Descriptors for WSIs Diagnosis," *Diagnostics*, vol. 12, no. 6, p. 1480, Jun. 2022, doi: https://doi.org/10.3390/diagnostics12061480.

[32] M. Liu, Y. He, M. Wu, and C. Zeng, "Breast Histopathological Image Classification Method Based on Autoencoder and Siamese Framework," *Information*, vol. 13, no. 3, p. 107, Mar. 2022, doi: https://doi.org/10.3390/info13030107.

[33] X. Li, C. Pan, H. Ling, and X. Li, "Unsupervised Domain Adaptation for Cross-domain Histopathology Image Classification," *Multimedia Tools and Applications*, Aug. 2023, doi: https://doi.org/10.1007/s11042-023-16400-y.

[34] P. Alirezazadeh, B. Hejrati, A. Monsef-Esfahani, and A. Fathi, "Representation learning-based unsupervised domain adaptation for classification of breast cancer histopathology images," *Biocybernetics and Biomedical Engineering*, vol. 38, no. 3, pp. 671–683, 2018, doi: https://doi.org/10.1016/j.bbe.2018.04.008.

[35] Y. Bai *et al.*, "Masked autoencoders with handcrafted feature predictions: Transformer for weakly supervised esophageal cancer classification," *Computer methods and programs in biomedicine*, vol. 244, pp. 107936–107936, Feb. 2024, doi https://doi.org/10.1016/j.cmpb.2023.107936.

[36] J. Ke, Y. Shen, Y. Lu, Y. Guo, and D. Shen, "Mine local homogeneous representation by interaction information clustering with unsupervised learning in histopathology images," vol. 235, pp. 107520–107520, Jun. 2023, doi: https://doi.org/10.1016/j.cmpb.2023.107520.

[37] J. Li *et al.*, "DARC: Deep adaptive regularized clustering for histopathological image classification," *Medical Image Analysis*, vol. 80, p. 102521, Aug. 2022, doi: https://doi.org/10.1016/j.media.2022.102521.

[38] J. Cai, S. Wang, and W. Guo, "Unsupervised embedded feature learning for deep clustering with stacked sparse auto-encoder," *Expert Systems with Applications*, vol. 186, p. 115729, Dec. 2021, doi: https://doi.org/10.1016/j.eswa.2021.115729.

[39] J. A. Hartigan and M. A. Wong, "Algorithm AS 136: A K-Means Clustering Algorithm," *Applied Statistics*, vol. 28, no. 1, p. 100, 1979, doi: https://doi.org/10.2307/2346830.

[40] D. T. Pham, S. S. Dimov, and C. D. Nguyen, "Selection of K in K-means clustering," *Proceedings of the Institution of Mechanical Engineers, Part C: Journal of Mechanical Engineering Science*, vol. 219, no. 1, pp. 103–119, Jan. 2005, doi: https://doi.org/10.1243/095440605x8298.

[41] A. Likas, N. Vlassis, and J. J. Verbeek, "The global k-means clustering algorithm," *Pattern Recognition*, vol. 36, no. 2, pp. 451–461, Feb. 2003, doi: https://doi.org/10.1016/s0031-3203(02)00060-2.

[42] A. M. Ikotun, A. E. Ezugwu, L. Abualigah, B. Abuhaija, and J. Heming, "K-means Clustering Algorithms: a Comprehensive Review, Variants Analysis, and Advances in the Era of Big Data," *Information Sciences*, vol. 622, no. 622, Dec. 2022, doi: https://doi.org/10.1016/j.ins.2022.11.139.

[43] P. Bradley, K. Bennett, and A. Demiriz, "Constrained K-Means Clustering," 2000. Available: http://machinelearning102.pbworks.com/f/ConstrainedKMeanstr-2000-65.pdf

[44] S. Na, L. Xumin, and G. Yong, "Research on k-means Clustering Algorithm: An Improved k-means Clustering Algorithm," *2010 Third International Symposium on Intelligent Information Technology and Security Informatics*, Apr. 2010, doi: https://doi.org/10.1109/iitsi.2010.74.

[45] K. P. Sinaga and M.-S. Yang, "Unsupervised K-Means Clustering Algorithm," *IEEE Access*, vol. 8, pp. 80716–80727, 2020, doi: https://doi.org/10.1109/access.2020.2988796.

[46] M. Ahmed, R. Seraj, and S. M. S. Islam, "The k-means Algorithm: A Comprehensive Survey and Performance Evaluation," *Electronics*, vol. 9, no. 8, p. 1295, Aug. 2020, doi: https://doi.org/10.3390/electronics9081295.

[47] S. Cascianelli *et al.*, "Dimensionality Reduction Strategies for CNN-Based Classification of Histopathological Images," *Smart innovation, systems and technologies*, pp. 21–30, May 2017, doi: https://doi.org/10.1007/978-3-319-59480-4_3.

[48] B. Liu, C. Liu, Y. Zhou, D. Wang, and Y. Dun, "An unsupervised chatter detection method based on AE and merging GMM and K-means," *Mechanical Systems and Signal Processing*, vol. 186, p. 109861, Mar. 2023, doi: https://doi.org/10.1016/j.ymssp.2022.109861.

[49] A. Bigdeli, A. Maghsoudi, and R. Ghezelbash, "Application of self-organizing map (SOM) and K-means clustering algorithms for portraying geochemical anomaly patterns in Moalleman district, NE Iran," *Journal of Geochemical Exploration*, vol. 233, p. 106923, Feb. 2022, doi: https://doi.org/10.1016/j.gexplo.2021.106923.

[50] N. Saeidi, H. Karshenas, B. Shoushtarian, S. Hatamikia, R. Woitek, and A. Mahbod, "Breast Histopathology Image Retrieval by Attention-based Adversarially Regularized Variational Graph Autoencoder with Contrastive Learning-Based Feature Extraction," *arXiv.org*, Jun. 10, 2024. https://arxiv.org/abs/2405.04211 (accessed Jul. 11, 2024).

[51] F. Cano, Charlems Alvarez-Jimenez, E. Romero, and A. Cruz-Roa, "Ensemble of Unsupervised Learned Image Representations Based On Variational Autoencoders for Lung Adenocarcinoma Subtype Differentiation," *2023 IEEE 20th International Symposium on Biomedical Imaging (ISBI)*, Apr. 2023, doi: https://doi.org/10.1109/isbi53787.2023.10230823.

[52] N. Arya, A. Mathur, S. Saha, and S. Saha, "Proposal of SVM Utility Kernel for Breast Cancer Survival Estimation," *IEEE/ACM Transactions on Computational Biology and Bioinformatics*, vol. 20, no. 2, pp. 1372–1383, Mar. 2023, doi: https://doi.org/10.1109/tcbb.2022.3198879.

[53] A. H. Abdulwahhab, Alaa Hussein Abdulaal, A. H. Thary Al-Ghrairi, Ali Abdulwahhab Mohammed, and Morteza Valizadeh, "Detection of epileptic seizure using EEG signals analysis based on deep learning techniques," *Chaos, solitons & fractals/Chaos, solitons and fractals*, vol. 181, pp. 114700–114700, Apr. 2024, doi: https://doi.org/10.1016/j.chaos.2024.114700.

[54] K. Simonyan and A. Zisserman, "Very Deep Convolutional Networks for Large-Scale Image Recognition," *arXiv.org*, Apr. 10, 2015. https://arxiv.org/abs/1409.1556

[55] F. A. Spanhol, L. S. Oliveira, C. Petitjean, and L. Heutte, "Breast cancer histopathological image classification using Convolutional Neural Networks," *2016 International Joint Conference on Neural Networks (IJCNN)*, Jul. 2016, doi: https://doi.org/10.1109/ijcnn.2016.7727519.

[56] S. Sharma, R. Mehra, and S. Kumar, "Optimised CNN in conjunction with efficient pooling strategy for the multi-classification of breast cancer," *IET Image Processing*, Dec. 2020, doi: https://doi.org/10.1049/ipr2.12074.

[57] A. H. Abdulaal, M. Valizadeh, M. C. Amirani, and A. F. M. Shahen Shah, "A self-learning deep neural network for classification of breast histopathological images," *Biomedical Signal Processing and Control*, vol. 87, p. 105418, Jan. 2024, doi: https://doi.org/10.1016/j.bspc.2023.105418.

[58] S. Kanimozhi and S. Priyadarsini, "Breast Cancer Histopathological Image Classification Using CNN and VGG-19," *2024 Third International Conference on Intelligent Techniques in Control, Optimization and Signal Processing (INCOS)*, Mar. 2024, doi: https://doi.org/10.1109/incos59338.2024.10527543.

[59] A. M. Zaalouk, G. A. Ebrahim, H. K. Mohamed, H. M. Hassan, and M. M. A. Zaalouk, "A Deep Learning Computer-Aided Diagnosis Approach for Breast Cancer," *Bioengineering*, vol. 9, no. 8, p. 391, Aug. 2022, doi: https://doi.org/10.3390/bioengineering9080391.

[60] Muhammad Shahzeb Khan *et al.*, "VGG19 Network Assisted Joint Segmentation and Classification of Lung Nodules in CT Images," *Diagnostics*, vol. 11, no. 12, pp. 2208–2208, Nov. 2021, doi: https://doi.org/10.3390/diagnostics11122208.

[61] Xiao Yu Tian, H. Daigle, and J. Han, "Feature Detection for Digital Images Using Machine Learning Algorithms and Image Processing," *Proceedings of the 6th Unconventional Resources Technology Conference*, Jan. 2018, doi: https://doi.org/10.15530/urtec-2018-2886325.

[62] P. Agarwal, A. Yadav, and P. Mathur, "Breast Cancer Prediction on BreakHis Dataset Using Deep CNN and Transfer Learning Model," *Lecture notes in networks and systems*, pp. 77–88, Nov. 2021, doi: https://doi.org/10.1007/978-981-16-2641-8_8.

[63] F. Bayram and A. Eleyan, "COVID-19 detection on chest radiographs using feature fusion based deep learning," *Signal, Image and Video Processing*, Jan. 2022, doi: https://doi.org/10.1007/s11760-021-02098-8.

[64] D. P. Kingma and M. Welling, "Auto-Encoding Variational Bayes," *arXiv.org*, Dec. 20, 2013. https://arxiv.org/abs/1312.6114

[65] R. Lopez, J. Regier, M. I. Jordan, and N. Yosef, "Information Constraints on Auto-Encoding Variational Bayes," *Neural Information Processing Systems*, 2018. https://proceedings.neurips.cc/paper/2018/hash/9a96a2c73c0d477ff2a6da3bf538f4f4-Abstract.html (accessed Jul. 11, 2024).

[66] G. W. Pulford, "From the Expectation Maximisation Algorithm to Autoencoded Variational Bayes," *arXiv.org*, May 04, 2021. https://arxiv.org/abs/2010.13551 (accessed Jul. 11, 2024).

[67] O. Kviman, R. Molén, A. Hotti, S. Kurt, ElviraV., and J. Lagergren, "Cooperation in the Latent Space: The Benefits of Adding Mixture Components in Variational Autoencoders," *proceedings. mlr.press*, Jul. 03, 2023. https://proceedings.mlr.press/v202/kviman23a.html (accessed Jul. 11, 2024).

[68] I. Cetin, M. Stephens, O. Camara, and M. A. González Ballester, "Attri-VAE: Attribute-based interpretable representations of medical images with variational autoencoders," *Computerized Medical Imaging and Graphics*, vol. 104, p. 102158, Mar. 2023, doi: https://doi.org/10.1016/j.compmedimag.2022.102158.

[69] X. Lin, Y. Li, J. Hsiao, C. Ho, and Y. Kong, "Catch Missing Details: Image Reconstruction With Frequency Augmented Variational Autoencoder," *openaccess.thecvf.com*, 2023. http://openaccess.thecvf.com/content/CVPR2023/html/Lin_Catch_Missing_Details_Image_Reconstruction_With_Frequency_Augmented_Variational_Autoencoder_CVPR_2023_paper.html (accessed Jul. 11, 2024).

[70] T. Sudak and S. Tschiatschek, "Posterior Consistency for Missing Data in Variational Autoencoders," *Lecture notes in computer science*, pp. 508–524, Jan. 2023, doi: https://doi.org/10.1007/978-3-031-43415-0_30.

[71] F. Mendonça, S. S. Mostafa, F. Morgado-Dias, and A. G. Ravelo-García, "On the Use of Kullback–Leibler Divergence for Kernel Selection and Interpretation in Variational Autoencoders for Feature Creation,"

Information, vol. 14, no. 10, p. 571, Oct. 2023, doi https://doi.org/10.3390/info14100571.

[72] D. Addo *et al.*, "EVAE-Net: An Ensemble Variational Autoencoder Deep Learning Network for COVID-19 Classification Based on Chest X-ray Images," *Diagnostics*, vol. 12, no. 11, pp. 2569–2569, Oct. 2022, doi: https://doi.org/10.3390/diagnostics12112569.

[73] P. Govender and V. Sivakumar, "Application of k-means and hierarchical clustering techniques for analysis of air pollution: A review (1980–2019)," *Atmospheric Pollution Research*, vol. 11, no. 1, pp. 40–56, Jan. 2020, doi: https://doi.org/10.1016/j.apr.2019.09.009.

[74] M. Kumagai, K. Komatsu, M. Sato, and H. Kobayashi, "Ising-Based Kernel Clustering," *Algorithms*, vol. 16, no. 4, p. 214, Apr. 2023, doi: https://doi.org/10.3390/a16040214.

[75] S. Bandyopadhyay, F. V. Fomin, P. A. Golovach, W. Lochet, N. Purohit, and K. Simonov, "How to find a good explanation for clustering?," *Artificial Intelligence*, vol. 322, p. 103948, Sep. 2023, doi: https://doi.org/10.1016/j.artint.2023.103948.

[76] Y. Sahu, A. Tripathi, R. K. Gupta, P. Gautam, R. K. Pateriya, and A. Gupta, "A CNN-SVM based computer-aided diagnosis of breast cancer using histogram K-means segmentation technique," *Multimedia Tools and Applications*, Sep. 2022, doi: https://doi.org/10.1007/s11042-022-13807-x.

[77] S. M. Javidan, A. Banakar, K. A. Vakilian, and Y. Ampatzidis, "Diagnosis of grape leaf diseases using automatic K-means clustering and machine learning," *Smart Agricultural Technology*, vol. 3, p. 100081, Feb. 2023, doi: https://doi.org/10.1016/j.atech.2022.100081.

[78] Hossain Shakhawat, Sakir Hossain, Alamgir Kabir, S. M. Hasan Mahmud, M. M. Manjurul Islam, and Faisal Tariq, "Review of Artifact Detection Methods for Automated Analysis and Diagnosis in Digital Pathology," *Artificial Intelligence for Disease Diagnosis and Prognosis in Smart Healthcare*, Jan. 01, 2023, doi: https://doi.org/10.1201/9781003251903

[79] S. Li, P. Kou, M. Ma, H. Yang, S. Huang, and Z. Yang, "Application of Semi-supervised Learning in Image Classification: Research on Fusion of Labeled and Unlabeled Data," *IEEE Access*, pp. 1–1, Jan. 2024, doi: https://doi.org/10.1109/access.2024.3367772.

[80] Alaa Hussein Abdulaal, Morteza Valizadeh, Baraa M. Albaker, Riyam Ali Yassin, Mehdi Chehel Amirani, and A. F. M. Shahen Shah, "Enhancing Breast Cancer Classification using a Modified GoogLeNet Architecture with Attention Mechanism," *Al-Iraqia Journal of Scientific Engineering Research*, vol. 3, no. 1, Mar. 2024, doi: https://doi.org/10.58564/ijser.3.1.2024.145.

[81] L. Cao, K. Pan, Y. Ren, R. Lu, and J. Zhang, "Multi-Branch Spectral Channel Attention Network for Breast Cancer Histopathology Image Classification," *Electronics*, vol. 13, no. 2, p. 459, Jan. 2024, doi: https://doi.org/10.3390/electronics13020459.

[82] Jia Rong Leow, Wee How Khoh, Ying Han Pang, and Hui Yen Yap, "Breast cancer classification with histopathological image based on machine learning," *International Journal of Electrical and Computer Engineering (IJECE)*, Oct. 05, 2023, doi: http://doi.org/10.11591/ijece.v13i5.pp5885-5897

[83] S. Garg and P. Singh, "Transfer Learning Based Lightweight Ensemble Model for Imbalanced Breast Cancer Classification," *IEEE/ACM Transactions on Computational Biology and Bioinformatics*, pp. 1–1, 2022, doi: https://doi.org/10.1109/tcbb.2022.3174091.

[84] H. Zhu *et al.*, "Deconv-transformer (DecT): A histopathological image classification model for breast cancer based on color deconvolution and transformer architecture," *Information Sciences*, vol. 608, pp. 1093–1112, Aug. 2022, doi: https://doi.org/10.1016/j.ins.2022.06.091.

[85] Y. Zou, J. Zhang, S. Huang, and B. Liu, "Breast cancer histopathological image classification using attention high-order deep network," *International Journal of Imaging Systems and Technology*, vol. 32, no. 1, pp. 266–279, Jul. 2021, doi: https://doi.org/10.1002/ima.22628.